FEMS Microbiology Ecology, 97, 2021, fiab052

doi: 10.1093/femsec/fiab052
Advance Access Publication Date: 30 March 2021
Research Article

RESEARCH ARTICLE

The association between initial adhesion and cyanobacterial biofilm development

Sara I. Faria[1,†,‡], Rita Teixeira-Santos[1,†,§], João Morais[2], Vitor Vasconcelos[2,3] and Filipe J. Mergulhão[1,*]

[1]LEPABE - Laboratory for Process Engineering, Environment, Biotechnology and Energy, Faculty of Engineering, University of Porto, Rua Dr. Roberto Frias, 4200–465, Porto, Portugal, [2]CIIMAR – Interdisciplinary Centre of Marine and Environmental Research, University of Porto, Terminal de Cruzeiros do Porto de Leixões, Avenida General Norton de Matos, S/N, 4450-208, Matosinhos, Portugal and [3]FCUP – Faculty of Sciences, University of Porto, Rua do Campo Alegre, 4069-007, Porto, Portugal

*Corresponding author: Department of Chemical Engineering, Faculty of Engineering, University of Porto, Rua Dr. Roberto Frias, 4200–465 Porto, Portugal. Tel: (+351) 225 081 668; Fax: (+351) 225 081 449; E-mail: filipem@fe.up.pt

One sentence summary: Initial cell adhesion assays revealed a high potential to estimate cyanobacterial biofilm development, allowing high throughput screening of marine coatings under different conditions and providing indications about the biofilm behaviour in a short time.

†These authors contributed equally to this work.

Editor: Julie Olson

‡Sara I. Faria, http://orcid.org/0000-0002-4819-1892
§Rita Teixeira-Santos, http://orcid.org/0000-0001-7546-9362

ABSTRACT

Although laboratory assays provide valuable information about the antifouling effectiveness of marine surfaces and the dynamics of biofilm formation, they may be laborious and time-consuming. This study aimed to determine the potential of short-time adhesion assays to estimate how biofilm development may proceed. The initial adhesion and cyanobacterial biofilm formation were evaluated using glass and polymer epoxy resin surfaces under different hydrodynamic conditions and were compared using linear regression models. For initial adhesion, the polymer epoxy resin surface was significantly associated with a lower number of adhered cells compared with glass (-1.27 $\times$ 10^5 cells.cm^{-2}). Likewise, the number of adhered cells was significantly lower (-1.16 $\times$ 10^5 cells.cm^{-2}) at 185 than at 40 rpm. This tendency was maintained during biofilm development and was supported by the biofilm wet weight, thickness, chlorophyll *a* content and structure. Results indicated a significant correlation between the number of adhered and biofilm cells ($r = 0.800$, $p < 0.001$). Moreover, the number of biofilm cells on day 42 was dependent on the number of adhered cells at the end of the initial adhesion and hydrodynamic conditions ($R^2 = 0.795$, $p < 0.001$). These findings demonstrate the high potential of initial adhesion assays to estimate marine biofilm development.

Keywords: coccoid cyanobacteria; initial adhesion; biofilm formation; antifouling surfaces; hydrodynamic conditions; marine biofouling

INTRODUCTION

The attachment of undesirable molecules and fouling organisms to submerged surfaces is known as marine biofouling (Selim *et al.* 2017; Rajeev *et al.* 2020). This process occurs spontaneously in marine ecosystems and may have several economic and environmental implications (Basu *et al.* 2020). Marine biofouling is detrimental to vessel hulls since the attached fouling organisms

Received: 19 November 2020; **Accepted:** 25 March 2021

exacerbate surface corrosion and increase frictional drag, resulting in higher maintenance and fuel consumption (Zecher *et al.* 2018; Rajeev *et al.* 2020; Tian *et al.* 2020). Similarly, biofouling can damage submerged marine facilities and underwater equipment such as measurement devices or sensors (Tian *et al.* 2020).

Besides the economic losses for marine industries, marine biofouling is associated with serious environmental issues. This process promotes the bio-invasion of exotic species when the fouling organisms travel in marine vessels (ships, yachts or sailing boats) between different geographic areas, which is aggravated at both community (species richness) and population (genetic diversity) levels by the intense shipping activity in ports (Lacoursière-Roussel *et al.* 2016; Neves *et al.* 2020). The negative impact of bio-invasion has motivated marine conservation entities to seek strategies to reduce the introduction and spread of fouling species in marine ecosystems and, in some countries, strict regulations have already been implemented to keep vessel hulls clean (McClay *et al.* 2015; Georgiades and Kluza 2017).

In general, the consequences of marine biofouling have stressed the need to develop and evaluate novel marine coatings aiming to control biofilm formation by microfouling organisms (e.g. cyanobacteria and diatoms) since this is the initial colonisation stage, building the basis for later settlement by macrofouling organisms (e.g. bryozoans, mollusks, polychaeta, tunicates, coelenterates or fungi) (Arrhenius *et al.* 2014).

Due to the vast number of fouling organisms and the diversity of biological factors underlying their attachment in the natural environment, the most reliable method for testing the antifouling (AF) performance of marine surfaces appears to be the immersion of samples in the ocean (Stafslien *et al.* 2011). However, sea trials require long periods to collect data, are dependent on samples' location and the time of year and may be ecologically toxic and expensive (Briand 2009; Salta *et al.* 2010; Zecher *et al.* 2018). Therefore, the first step for testing new AF coatings usually consists of exposing them to microfouling organisms under laboratory conditions that mimic the marine environments and to analyse different biofilm parameters (e.g. number of cells, wet weight and thickness) (Zecher *et al.* 2018; Romeu *et al.* 2019; Faria *et al.* 2020; Romeu *et al.* 2020). Since numerous extrinsic factors may affect the success of an AF coating, including the microorganisms, temperature and hydrodynamic conditions (Faria *et al.* 2020), it is important to test its efficacy against a broad spectrum of fouling organisms and marine conditions to obtain a more insightful evaluation (Briand 2009). Although several laboratory assays provide the first indications about AF performance and allow a better understanding of the dynamics of biofilm formation, they may be laborious and time-consuming, requiring on average 6 weeks to provide representative results of a real scenario (Zecher *et al.* 2018; Romeu *et al.* 2019). Thus, considering these limitations, the efficacy of AF marine coatings should first be screened before carrying out extensive laboratory tests. Certain adhesion and biofilm formation assays (2–48 h) have been developed for screening AF coatings (Leroy *et al.* 2007; Salta *et al.* 2010; Stafslien *et al.* 2011) and some of them showed a correlation with field assays (Stafslien *et al.* 2007; Briand 2009). Most of these assays are based on the enumeration of the attached cells by direct counting under a microscope after their staining (Leroy *et al.* 2007; Briand 2009; Salta *et al.* 2010) or on the spectrophotometric or fluorometric quantification of chlorophyll (Briand 2009). Cell staining usually requires several methodological steps (e.g. cell fixation, staining and washing) to improve analysis specificity and sensitivity, thus increasing the time to results and costs (Leroy *et al.* 2007; Briand 2009; Salta *et al.* 2010). In turn, the chlorophyll quantification may only be applied to chlorophyll-producing organisms (Briand 2009; Stafslien *et al.* 2011). Besides, most laboratory assays are conducted under static conditions (Stafslien *et al.* 2007; Briand 2009; Salta *et al.* 2010), which can influence AF performance (Nolte *et al.* 2017, 2018). Thus, although these assays are very useful as screening tools, it is necessary to develop rapid, inexpensive and more accurate and simple methods to perform alternative short-term assays.

In the present study, the association between initial adhesion and biofilm formation was investigated, aiming to evaluate the potential of short-time adhesion assays to estimate biofilm development and, consequently, the antifouling efficacy of a given surface. For this purpose, the initial adhesion and biofilm formation of three coccoid cyanobacteria isolated from different geographic areas were evaluated using different surfaces (glass and a polymer epoxy resin) and hydrodynamic conditions (40 and 185 rpm agitation). Since cyanobacteria are some of the most dominant bacterial phyla colonising different surfaces at diverse sampling locations (de Carvalho 2018; Angelova *et al.* 2019), particularly in the early stages of colonisation (Azevedo *et al.* 2020), these microfoulers were chosen for the current study.

MATERIALS AND METHODS

Surfaces preparation

Cyanobacterial adhesion and biofilm formation were studied using two model surfaces, glass and a polymer epoxy resin. Glass surfaces are commonly found in the underwater windows of boats, flotation spheres, moored buoys, underwater cameras and measuring devices or sensors (Taylor 1996; King *et al.* 2006), while polymer epoxy resins are used to coat the hulls of small recreation vessels, including powerboats, yachts and sailing boats (Taylor 1996; Blain *et al.* 2004). Glass coupons (1 × 1 cm; Vidraria Lousada Lda, Lousada, Portugal) were cleaned and disinfected by immersion in a 2% (v/v) TEGO 2000® solution (an amphoteric disinfectant; JohnsonDiversey, Northampton, UK) for 20 min at 150 rpm (Meireles *et al.* 2017; Gomes *et al.* 2018). Then the coupons were washed with sterile distilled water to remove possible remains of the disinfectant solution, air-dried and autoclaved at 121°C for 15 min (Azevedo *et al.* 2006). In turn, the polymer epoxy resin surfaces were prepared from the cleaned and sterilised glass surfaces. Glass coupons were gently coated with 150 μL of the polymer epoxy resin (HB Química, Matosinhos, Portugal; composition detailed in Supporting information, S1) and dried in two sequential steps: (i) 12 h at room temperature (25 ± 2°C), and (ii) 3h at 60°C, according to the instructions from the manufacturer. Dried coated coupons were immersed in 70% (v/v) ethanol (VWR International S.A.A., Fontenay-sous-Bois, France) for 20 min to sterilise them.

Before experiments, the initial weight of glass and polymer epoxy resin coupons was registered.

Cyanobacterial strains and growth conditions

Three coccoid cyanobacteria strains from the Blue Biotechnology and Ecotoxicology Culture Collection (LEGE-CC), deposited at the Interdisciplinary Centre of Marine and Environmental Research (CIIMAR), Porto, Portugal, were included in this study. *Synechocystis salina* LEGE 00041 (order Chroococcales) was originally isolated from a seawater sample, collected in June 2000, at Espinho beach (41.00 847 N 8.646 958 W) located on the north coast of Portugal; *Synechocystis salina* LEGE 06155 (order

Chroococcales) was obtained from a rock surface scraping of a tide pool, collected in November 2006, at São Bartolomeu do Mar beach (41.57 377 N 8.798 558 W) located in Esposende, Portugal; and *Cyanobium* sp. LEGE 06097 (order Synechococcales) was isolated from the intertidal zone, on green macroalga, collected in July 2006, at Martinhal beach (37.01 869 N 8.926 714 W) located in Vila do Bispo, Portugal (Ramos *et al.* 2018).

Cyanobacterial cells have grown in Z8 broth medium supplemented with 25 mg.mL^{-1} of synthetic sea salts (Tropic Marin) and B12 vitamin (Sigma Aldrich, Merck, Saint Loius, MO, USA) (Kotai 1972). Cultures were incubated under 14 h light (10–30 mol photon m^{-2} s^{-1}, λ = 380–700 nm)/10 h dark cycles at 25°C.

Thermodynamic characterisation

The hydrophobicity of the surfaces and cyanobacteria cells was evaluated by contact angle measurement. For cyanobacteria, cell suspensions containing 1 × 10^9 cells.mL^{-1} were prepared and analysed following the protocol developed by Busscher *et al.* (1984). The contact angles of both materials and cyanobacteria cells were determined automatically at 25 ± 2°C by the sessile drop method in a contact angle meter (Dataphysics OCA 15 Plus, Germany) using water, formamide and α-bromonaphthalene as reference liquids, in three independent assays. For each experiment, at least 25 measurements were performed.

Based on the van Oss approach (Oss 1994), the total surface energy (γ^{TOT}) of a pure substance results from the sum of the apolar Lifshitz-van der Waals component of the surface-free energy (γ^{LW}) and the polar Lewis acid-base component (γ^{AB}):

$$\gamma^{TOT} = \gamma^{LW} + \gamma^{AB} \quad (1)$$

The polar AB component comprises the electron acceptor γ^+ and electron donor γ^- parameters and is given by:

$$\gamma^{AB} = 2\sqrt{\gamma^+\gamma^-} \quad (2)$$

The surface energy components of a solid surface (s) are obtained by measuring the contact angles (θ) with three different liquids (l) with known surface tension components (Janczuk *et al.* 1993), followed by the simultaneous resolution of three equations of the type:

$$(1 + \cos\theta)\gamma_l = 2\left(\sqrt{\gamma_s^{LW}\gamma_l^{LW}} + \sqrt{\gamma_s^+\gamma_l^-} + \sqrt{\gamma_s^+\gamma_l^-}\right) \quad (3)$$

Water contact angles (θ_w) indicate the surface hydrophobicity ($\theta_w < 90°$ indicates that a surface is hydrophilic, while $\theta_w > 90°$ indicates that it is hydrophobic) (Ma *et al.* 2007).

The degree of hydrophobicity of a given surface is expressed as the free energy of interaction (ΔG, mJ.m^{-2}) between two entities of that surface immersed in polar liquid (such as water (w) as a model solvent). Therefore, ΔG is calculated using the equation:

$$\Delta G = -2\left(\sqrt{\gamma_s^{LW}} - \sqrt{\gamma_w^{LW}}\right)^2 - 4\left(\sqrt{\gamma_s^+\gamma_w^-} + \sqrt{\gamma_s^-\gamma_w^+} - \sqrt{\gamma_s^+\gamma_s^-} - \sqrt{\gamma_w^+\gamma_w^-}\right) \quad (4)$$

According to this approach, if the interaction between the two entities is stronger than the interaction of each one with water ($\Delta G < 0$ mJ.m^{-2}), the material is considered to be hydrophobic (i.e. the free energy of the interaction is attractive); on the contrary, if $\Delta G > 0$ mJ.m^{-2}, the material is hydrophilic (i.e. the free energy of the interaction is repulsive) (Bayoudh *et al.* 2006).

When studying the interaction (free energy of adhesion) between the surface (s) and cyanobacteria cells (b), the total interaction energy ΔG^{Adh}, can be expressed as:

$$\Delta G^{Adh} = \gamma_{sb}^{Lw} - \gamma_{sw}^{Lw} - \gamma_{bw}^{Lw} + 2\left[\sqrt{\gamma_w^+}\left(\sqrt{\gamma_s^-} + \sqrt{\gamma_b^-} - \sqrt{\gamma_w^-}\right) + \sqrt{\gamma_w^-}\left(\sqrt{\gamma_s^+} + \sqrt{\gamma_b^+} - \sqrt{\gamma_w^+}\right) - \sqrt{\gamma_s^+\gamma_b^-} - \sqrt{\gamma_s^-\gamma_b^+}\right] \quad (5)$$

Thermodynamically, if $\Delta G^{Adh} < 0$ mJ.m^{-2}, the adhesion of cyanobacteria to the material is favoured; in opposition, the adhesion is not favourable when $\Delta G^{Adh} > 0$ mJ.m^{-2}.

Initial adhesion assays

Cyanobacterial adhesion assays were performed using 12-well plates (VWR International, Carnaxide, Portugal) under previously optimised conditions (Romeu *et al.* 2019). Firstly, microplates were UV-sterilised for 30 min. Then the coupons (glass and polymer epoxy resin) were fixed to the microplate wells using transparent double-sided adhesive tape and inoculated with 3 mL of cyanobacterial suspension at a concentration of 1 × 10^8 cells.mL^{-1} (as previously described). Microplates were incubated at 25°C in an orbital shaker with a 25 mm diameter (Agitorb 200ICP, Norconcessus, Ermesinde, Portugal) at 40 and 185 rpm, under a light cycle (10–30 mol photons m^{-2} s^{-1}). Based on computational fluid dynamic studies performed using this type of incubator, a shaking frequency of 40 rpm corresponds to an average shear rate of 4 s^{-1} and a maximum of 11 s^{-1}, while 185 rpm corresponds to an average shear rate of 40 s^{-1} and a maximum of 120 s^{-1} (Romeu *et al.* 2019). As it is known that lower shear rates promote marine biofouling (Minchin and Gollasch 2003; Flemming *et al.* 2009) and the estimated shear rate for a ship in a harbour is 50 s^{-1} (Bakker *et al.* 2003), both shaking frequencies were studied.

Since in marine environments, the bacterial adhesion occurs within the first 24 h (Brian-Jaisson 2014; Amara *et al.* 2018), the initial adhesion assays were performed during 450 min (7.5 h). Every 90 min, two coupons for each experimental condition ([i] glass at 40 rpm; [ii] glass at 185 rpm; [iii] polymer epoxy resin at 40 rpm; and [iv] polymer epoxy resin at 185 rpm) were removed and analysed concerning the number of adhered cells. For this purpose, each coupon was immersed in 2 mL of 8.5 mg.mL^{-1} sodium chloride solution and vortexing took place for 3 min to detach cyanobacteria cells. Then 10 μL of each cell suspension was placed on each side of a Neubauer chamber and observed with a brightfield microscope (Nikon Eclipse LV100 microscope; Nikon Corporation, Tokyo, Japan). Additionally, the coupons were also observed under the microscope to confirm complete cell detachment.

Experiments were performed in duplicate and in two independent assays.

Biofilm formation assays

Biofilm formation was performed as described in the section above under alternate light cycles of 14 h light (10–30 mol photons m^{-2} s^{-1})/10 h dark, and followed for 6 weeks (42 days) since this period corresponds on average to half of the minimal economically viable interval accepted for the maintenance of underwater systems (Blain *et al.* 2004) and hull cleaning (Akinfijevs *et al.* 2007; Schultz *et al.* 2011). During this period, the culture medium was replaced twice a week. On days 1, 2, 4, 7, 14, 21, 28, 35 and 42, two coupons of each experimental condition were removed and gently rinsed in a sterile sodium chloride solution (8.5 $mg.mL^{-1}$) to remove loosely attached cyanobacteria. Afterwards, coupons were analysed concerning the number of biofilm cells, biofilm wet weight and thickness and chlorophyll *a* content. Additionally, on day 42, the biofilm structure was analysed by optical coherence tomography (OCT).

Biofilm experiments were performed in duplicate and in two independent assays.

Biofilm cell counting

For cell counting, coupons were dipped in 2 mL of 8.5 $mg.mL^{-1}$ sodium chloride solution and vortexed for 3 min at maximum power. Then 10 μL of cellular suspension was placed on each side of the Neubauer Camera and observed using a Nikon Eclipse LV100 microscope. To confirm complete cyanobacterial detachment, coupons were analysed under the microscope.

Biofilm wet weight

To assess the biofilm wet weight, coupons were removed from the wells with a tweezer and weighed. The biofilm wet weight was determined by the difference between the initial weight of the coupon (before inoculation) and the weight measured on the sampling day.

Biofilm thickness

Biofilm thickness was determined using a Nikon Eclipse LV100 microscope coupled to a joystick (Prior Scientific Ltd, Cambridge, UK) connected to a camera (Nikon digital sight DS-RI 1, Japan) and analysed using NIS-Elements AR 4.13.05 software. For each coupon, a minimum of five fields was analysed to obtain accurate and reproducible results.

Chlorophyll *a* quantification

Cyanobacteria detached from coupons were harvested by centrifugation (3202 x g, for 5 min at room temperature) and the supernatant discarded. The protocol for chlorophyll *a* extraction was performed in the absence of light because these pigments are light sensitive (Romeu *et al.* 2019). Briefly, 2 mL of 99.8% methanol was added to the pellet and incubated at 4°C for 24 h to obtain the maximal chlorophyll *a* extraction. The absorbance at 750 nm (turbidity), 665 nm (chlorophyll *a*) and 652 nm (chlorophyll *b*) was determined through a V-1200 spectrophotometer (VWR International China Co., Ltd, Shanghai, China). The chlorophyll *a* concentration ($\mu g.cm^{-2}$) was calculated using the following equation (Porra *et al.* 1989).

$$Chla\ (\mu g.mL^{-1}) = 16.29 \times A^{665} - 8.54 \times A^{652} \quad (6)$$

OCT

On day 42, biofilm structures were analysed by OCT using a Thorlabs Ganymede instrument (Thorlabs GmbH, Dachau, Germany) with a central wavelength of 930 nm. After washing, the plate wells were filled with 3 mL of sterile sodium chloride solution (8.5 $mg.mL^{-1}$) and biofilms formed on coupons were imaged. The captured volume was 3.66 × 1.52 × 2.98 mm^3 (509 × 313 × 1024 pixels). Since biofilms are mainly composed of water (Telegdi *et al.* 2016), the refractive index was set to 1.40, close to the refractive index of water (1.33).

For each coupon, 2D imaging was performed in a minimum of five fields to ensure the accuracy and reproducibility of the results.

Statistical analysis

Descriptive statistics were used to calculate the mean and standard deviations for the contact angles, number of adhered cells and different biofilm parameters (number of biofilm cells, biofilm wet weight, thickness and chlorophyll *a* content).

Linear regression models (LRMs) between the number of cells and the independent variables (tested surfaces and hydrodynamic conditions) were performed for initial adhesion and biofilm formation. Models were adjusted for strain and incubation periods.

The correlation between the adhered cells at 7.5 h and biofilm cells on day 42 was determined using the Pearson correlation coefficient (*r*). In addition, the association between the number of biofilm cells registered on day 42 and the number of adhered cells at 7.5 h, surface and hydrodynamic conditions (independent variables) was also estimated using a LRM adjusted for strain.

LRMs were also applied between the biofilm wet weight, thickness and chlorophyll *a* content and the independent variables. Models were adjusted for strain and incubation periods.

For all LRMs, glass and 40 rpm were used as the reference conditions. Results were presented as beta estimates (β) and the corresponding 95% confidence intervals (95% CI). Significant results were considered for $p < 0.05$. Data analysis was performed using IBM SPSS Statistics version 24.0 for Windows (IBM SPSS, Inc., Chicago, IL, USA).

RESULTS

Thermodynamic analysis

The hydrophobicity of the surfaces and cyanobacterial cells was evaluated by contact angle measurement and based on the method of van Oss et al. (1994). Table 1 presents the thermodynamic analysis for the tested materials and cyanobacterial cells. Water contact angle (θ_w) values indicated that glass is hydrophilic ($\theta_w = 39.459 \pm 3.505°$, [$\theta_w < 90°$]), whereas the polymer epoxy resin surface is slightly hydrophobic ($\theta_w = 90.194 \pm 4.256°$, [$\theta_w > 90°$]). In turn, the free energy of interaction also demonstrated the hydrophilic behaviour of glass ($\Delta G = 19.383$ $mJ.m^{-2}$, [$\Delta G > 0$ $mJ.m^{-2}$]) and the hydrophobicity of polymer

Table 1. Contact angle measurements, surface tension parameters and free energy of interaction of cyanobacterial strains and tested surfaces.

	Contact angle (°)			Surface tension parameters (mJ.m^{-2})				
	Water	Formamide	α-Bromonaphtalene	γ_s^{LW}	γ_s^{AB}	γ_s^{+}	γ_s^{-}	ΔG
Surface								
Glass	39.459 ± 3.505	37.277 ± 4.584	48.065 ± 4.122	30.893	15.653	1.487	41.192	19.383
Polymer epoxy resin	90.194 ± 4.256	69.567 ± 4.292	42.147 ± 3.826	33.661	0.106	0.001	3.211	– 67.983
Microorganism								
S. salina LEGE 00041	38.085 ± 4.310	53.432 ± 3.280	37.261 ± 4.501	35.800	0	0	61.008	52.315
Cyanobium sp. LEGE 06097	25.698 ± 3.575	34.226 ± 4.376	31.168 ± 2.777	38.222	7.233	0.232	56.384	40.355
S. salina LEGE 06155	19.113 ± 3.498	35.418 ± 4.212	39.655 ± 4.336	34.771	9.559	0.360	63.532	48.980

Values represent the average value ± SD from three independent contact angle measurements.
γ_s^{LW}—apolar component; γ_s^{AB}—polar component; γ_s^{+} and γ_s^{-}—surface tension parameters; ΔG—free surface energy.

Table 2. Free energy of the interaction between cyanobacterial strains and tested surfaces.

	ΔG^{Adh} (mJ.m^{-2})	
Microorganism	**Glass**	**Polymer epoxy resin**
S. salina LEGE 00041	32.633	– 7.994
Cyanobium sp. LEGE 06097	28.649	– 8.356
S. salina LEGE 06155	32.372	– 2.276

ΔG^{Adh}—free energy of adhesion.

epoxy resin surfaces ($\Delta G = -67.983$ mJ.m^{-2}, [$\Delta G < 0$ mJ.m^{-2}]). Concerning the cyanobacterial cells, water contact angles determined by the sessile drop method in a contact angle meter and the free energy of interaction showed that *Synechocystis salina* LEGE 00041 is relatively more hydrophobic than the other cyanobacteria ($\theta_{w\ 00041} = 38.085 \pm 4.310^\circ > \theta_{w\ 06097} = 25.698 \pm 3.575^\circ > \theta_{w\ 06155} = 19.113 \pm 3.498^\circ$; $\Delta G_{00041} = 52.315$ mJ.m^{-2} > $\Delta G_{06155} = 48.980$ mJ.m^{-2} > $\Delta G_{061097} = 40.355$ mJ.m^{-2}).

The free energy of adhesion (ΔG^{Adh}) calculated for the two surfaces is presented in Table 2. ΔG^{Adh} values obtained for the different cyanobacteria strains were very similar and indicated that the cell adhesion on the polymer epoxy resin is thermodynamically favourable ($\Delta G^{Adh} < 0$ mJ.m^{-2}), while on glass it is unfavourable ($\Delta G^{Adh} > 0$ mJ.m^{-2}).

Initial adhesion and cyanobacterial biofilm formation

The number of adhered and biofilms cells were determined for 7.5 h and 42 days, respectively, by direct counting in a Neubauer Camera using a microscope. Regardless of the surface or hydrodynamic condition, *S. salina* LEGE 00041 exhibited on average a higher number of adhered cells ($3.06 \times 10^6 \pm 5.40 \times 10^5$ cells.cm^{-2}) than *Cyanobium* sp. LEGE 06155 ($6.20 \times 10^2 \pm 6.87 \times 10^2$ cells.cm^{-2}) and *S. salina* LEGE 06097 ($4.95 \times 10^2 \pm 6.02 \times 10^2$ cells.cm^{-2}) (Fig. 1.1a). After 42 days of biofilm formation, although the number of biofilm cells had increased, this trend was kept constant with *S. salina* LEGE 00041, reaching a mean of $3.84 \times 10^8 \pm 5.83 \times 10^8$ cells.cm^{-2}, and *Cyanobium* sp. LEGE 06097 and *S. salina* LEGE 06155, reaching a mean of $3.71 \times 10^3 \pm 6.04 \times 10^3$ and $5.92 \times 10^3 \pm 9.89 \times 10^3$ cells.cm^{-2}, respectively (Fig. 1.1b).

Surface effect on cell adhesion and biofilm formation

For the study of the surface effect on cell adhesion and biofilm formation, cyanobacteria cells were exposed to the glass and polymer epoxy surfaces for 7.5 h and 42 days, respectively, and the number of adhered cells was quantified for each experimental point. The mean adhered cyanobacteria cells on both surfaces is represented in Fig. 1.2a. Regarding the surfaces, all cyanobacteria strains had a higher number of adhered cells on glass than on the polymer epoxy resin surface. *Cyanobium* sp. LEGE 06097 and *S. salina* LEGE 06155 strains displayed similar behaviour, reaching a mean value of $6.42 \times 10^2 \pm 7.27 \times 10^2$ and $5.41 \times 10^2 \pm 6.47 \times 10^2$ cell.cm^{-2} on glass, respectively, and a mean of $5.98 \times 10^2 \pm 6.52 \times 10^2$ and $4.49 \times 10^2 \pm 5.59 \times 10^2$ cell.cm^{-2} on the polymer epoxy resin, respectively. In the case of *S. salina* LEGE 00041, although the differences are subtle, the number of cells adhered on glass was also higher than on the polymer epoxy resin surfaces ($3.25 \times 10^6 \pm 5.57 \times 10^5$ vs. $2.87 \times 10^6 \pm 4.54 \times 10^5$ cell.cm^{-2}). The same pattern was verified for cyanobacterial biofilms formed on glass and the polymer epoxy resin surfaces for 42 days. *Cyanobium* sp. LEGE 06097 and *S. salina* LEGE 06155 reached a mean value of $5.01 \times 10^3 \pm 7.68 \times 10^3$ and $7.88 \times 10^3 \pm 1.22 \times 10^4$ cells.cm^{-2} on glass, respectively, and a mean of $2.41 \times 10^3 \pm 3.32 \times 10^3$ and $3.96 \times 10^3 \pm 6.27 \times 10^3$ cells.cm^{-2} on the polymer epoxy resin surface, respectively (Fig. 1.2b). Likewise, the higher biofilm-forming *S. salina* LEGE 00041 presented a higher number of biofilm cells on glass ($4.26 \times 10^8 \pm 6.70 \times 10^8$ cells.cm^{-2}) than on the polymer epoxy resin surface ($3.42 \times 10^8 \pm 4.82 \times 10^8$ cells.cm^{-2}).

Hydrodynamic effect on cell adhesion and biofilm formation

For the study of the hydrodynamic effect on cell adhesion and biofilm formation, cyanobacteria cells were exposed to both glass and polymer epoxy surfaces under 40 and 185 rpm for 7.5 h and 42 days, respectively, and the number of adhered cells was quantified for each experimental point. Regarding the hydrodynamic conditions, the mean adhered cyanobacteria cells registered for two hydrodynamic conditions is represented in Fig. 1.3a. For *Cyanobium* sp. LEGE 06097, the mean number of adhered cells at 40 rpm was $5.17 \times 10^2 \pm 6.61 \times 10^2$ cells.cm^{-2}, while at 185 rpm it was $7.23 \times 10^2 \pm 7.05 \times 10^2$ cells.cm^{-2}. In opposition, *S. salina* LEGE 06155 reached a mean of $7.64 \times 10^2 \pm 7.25 \times 10^2$ cells.cm^{-2} at 40 rpm and $2.26 \times 10^2 \pm$

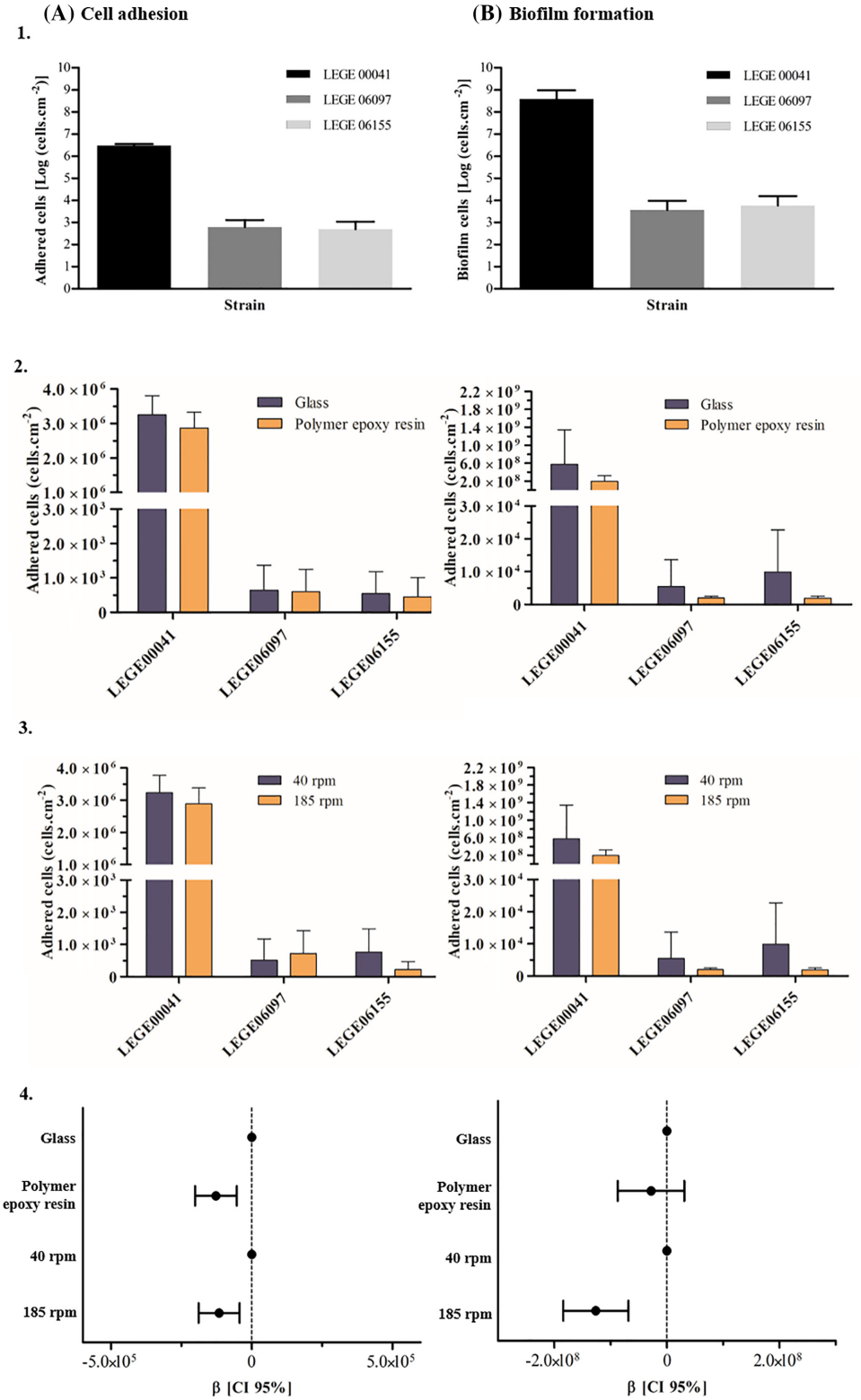

Figure 1. Association between initial cell adhesion and biofilm formation of three cyanobacteria strains (*Synechocystis salina* LEGE 00041, *S. salina* LEGE 06155 and *Cyanobium* sp. LEGE 06097) on glass and polymer epoxy resin surfaces under different hydrodynamic conditions. Mean of the cumulative number of cyanobacterial cells attached on glass and polymer epoxy resin surfaces at 40 and 185 rpm for cell adhesion (1**A**) and biofilm formation (1**B**) assays. Bar charts represent the mean of LEGE 00041, LEGE 06155 and LEGE 06097 attached cells on glass and polymer epoxy resin surfaces obtained for cell adhesion (2**A**) and biofilm formation (2**B**) assays, and the mean of LEGE 00041, LEGE 06155 and LEGE 06097 attached cells under 40 and 185 rpm registered for cell adhesion (3**A**) and biofilm formation (3**B**) assays. Linear regression models (LRMs) between the number of cells and the independent variables performed for initial adhesion (4**A**) and biofilm formation (4**B**). Glass and 40 rpm were used as the reference conditions. LRMs were adjusted for strain and incubation periods. Results are presented as beta estimates (β) and the corresponding 95% confidence interval (CI 95%).

2.45×10^2 cells.cm^{-2} at 185 rpm. Also, *S. salina* LEGE 00041 registered a higher number of adhered cells at 40 than at 185 rpm ($3.23 \times 10^6 \pm 5.36 \times 10^5$ vs. $2.89 \times 10^6 \pm 4.92 \times 10^5$ cells.cm^{-2}). In turn, cyanobacteria biofilms developed for 42 days presented a higher number of cells at low shear forces (Fig. 1.3b). *Synechocystis salina* LEGE 06155 and *S. salina* LEGE 00041 kept constant the pattern verified for adhesion assays, reaching a mean of $9.93 \times 10^3 \pm 1.28 \times 10^4$ and $5.73 \times 10^8 \pm 7.73 \times 10^8$ cells.cm^{-2} at 40 rpm, respectively, and a mean of $1.91 \times 10^3 \pm 5.84 \times 10^2$ and $1.95 \times 10^8 \pm 1.22 \times 10^8$ cells.cm^{-2} at 185 rpm, respectively. For *Cyanobium* sp., biofilms developed at 40 rpm also presented a higher number of cells ($5.46 \times 10^3 \pm 8.18 \times 10^3$ cells.cm^{-2}) than those developed at 185 rpm ($1.97 \times 10^3 \pm 5.70 \times 10^2$ cells.cm^{-2}).

Association between initial cell adhesion and biofilm development

To evaluate the influence of surface properties and hydrodynamic conditions on the number of adhered cells, LRMs were performed for initial adhesion and biofilm formation. In general, for initial adhesion, the polymer epoxy resin surface was significantly associated with a lower number of adhered cyanobacteria cells compared with the glass surface (-1.27×10^5 cells.cm^{-2} [-2.01×10^5: -5.29×10^4]) (Fig. 1.4a). Likewise, for the higher shear force, the number of adhered cells was significantly lower (-1.16×10^5 cells.cm^{-2} [-1.88×10^5: -4.31×10^4]) compared with the lower shear force (Fig. 1.4a). For biofilm formation, the polymer epoxy resin was also associated with a lower number of cells (-2.79×10^7 cells.cm^{-2} [-8.70×10^7: 3.13×10^7]) compared with glass (Fig. 1.4b). Although this association was not significant, the tendency verified for initial adhesion was maintained during biofilm formation. Concerning the hydrodynamic conditions, the high shear force was significantly associated with a lower number of cyanobacteria biofilm cells compared with the low shear force (-1.26×10^8 cells.cm^{-2} [-1.84×10^8: -6.81×10^7]) (Fig. 1.4b).

Additionally, the correlation between the number of adhered cells after 7.5 h and biofilm cells on day 42 was determined. Regardless of the surface or hydrodynamic conditions, there is a significant correlation between the number of adhered cells and biofilm cells obtained in the last sampling point for each assay ($r = 0.800$, $p < 0.001$). Data also indicated that the number of biofilm cells observed on day 42 depends on the number of adhered cells at the end of initial adhesion (7.5 h) and hydrodynamic conditions ($R^2 = 0.795$, $p < 0.001$; Supporting information, S2). Additionally, the surface was not significantly associated with the number of biofilm cells on day 42 ($p = 0.111$), despite playing a significant role in initial adhesion ($p = 0.001$).

Biofilm parameters analysis

LRMs were applied to evaluate the effect of surface properties and hydrodynamic conditions on biofilm wet weight and thickness and chlorophyll *a* content. Considering the biofilm parameters analysis, cyanobacterial biofilms formed on the polymer epoxy resin surface were significantly associated with a lower biofilm wet weight (-4.62 mg [-7.32: -1.92]), thickness (-14.22 μm [-19.57: -8.86]) and chlorophyll *a* content (-0.35 μg.mL^{-1} [-0.55: -0.14]) compared with those developed on glass (Fig. 2). In turn, cyanobacteria biofilms formed at 185 rpm were also associated with a lower biofilm wet weight (-2.74 mg [-5.42: -0.05]), thickness (-16.78 μm [-21.89: -11.66]) and chlorophyll *a* content (-0.78 μg.mL^{-1} [-0.97: -0.59]) compared with those developed at 40 rpm (Fig. 2).

Biofilm structure analysis

Cyanobacterial biofilm structures were evaluated on day 42 using OCT (Fig. 3). Regardless of shear forces, biofilms formed on polymer epoxy resin surfaces (Fig. 3.1–3.3c and d) exhibited fewer cells and lower thickness than those developed on glass (Fig. 3.1–3.3a and b). In addition, for both glass and polymer epoxy resin surfaces, biofilms formed at 185 rpm (Fig. 3.1–3.3b and d) presented a less developed structure than at 40 rpm (Fig. 3.1–3.3a and c). These results were verified for the three cyanobacteria strains.

DISCUSSION

Our study demonstrated that the cyanobacteria behaviour observed for the initial adhesion assays (7.5 h) remained constant during biofilm development (42 days). An association between cell adhesion and biofilm formation was observed for the three cyanobacteria isolates tested using glass and polymer epoxy resin surfaces at 40 and 185 rpm. Results revealed the potential of short-time adhesion assays (7.5 h) to estimate the biofilm formation under different conditions over 42 days and to provide important insights about the antifouling performance of marine coatings. Indeed, the tendency verified on initial adhesion assay regarding the cell adhesion on glass and polymer epoxy resin surfaces and at different hydrodynamic conditions was maintained during cyanobacterial biofilm development and was supported by analysis of the biofilm wet weight, thickness, chlorophyll *a* content and structure. Furthermore, the number of biofilm cells on day 42 was significantly dependent on the number of adhered cells after 7.5 h.

The majority of available short-term adhesion methods involve the incubation of a monoculture of microfoulers with a coated surface to allow cell attachment for 2–48 h followed by the enumeration of the attached cells by direct counting under a microscope, by staining cells or nucleic acids with dyes, or by spectrophotometric or fluorometric quantification of chlorophyll (Leroy *et al.* 2007; Briand 2009; Salta *et al.* 2010; Stafslien *et al.* 2011; Wendt 2017). The staining of attached cells requires several additional steps to increase their specificity and sensitivity (e.g. cell fixation, staining and washing) (Stafslien *et al.* 2011), making assays more laborious and expensive and increasing the time to results, while the chlorophyll quantification may only be applied to chlorophyll-producing organisms. Although some of these assays correlate with field assays (Stafslien *et al.* 2007; Briand 2009) and are useful screening tools for AF coatings, the initial adhesion assay proposed in this study is relatively rapid (7.5 h), inexpensive and easy to perform since it does not require specific dyes and additional staining steps and, based on our results, displays high accuracy. However, although this approach displayed promising results, it is important to highlight that the conditions and materials evaluated in this study are not representative of a real scenario and more tests to assess its correlation with sea trials are needed.

Similar to the results obtained in these short-term assays, previous studies demonstrated that *Escherichia coli* initial adhesion on different biomedical materials was able to predict biofilm formation for a 24-h period (Gomes *et al.* 2015; Lopez-Mila *et al.* 2018; Alves *et al.* 2020). Altogether, these findings suggest that initial microbial adhesion may provide important cues

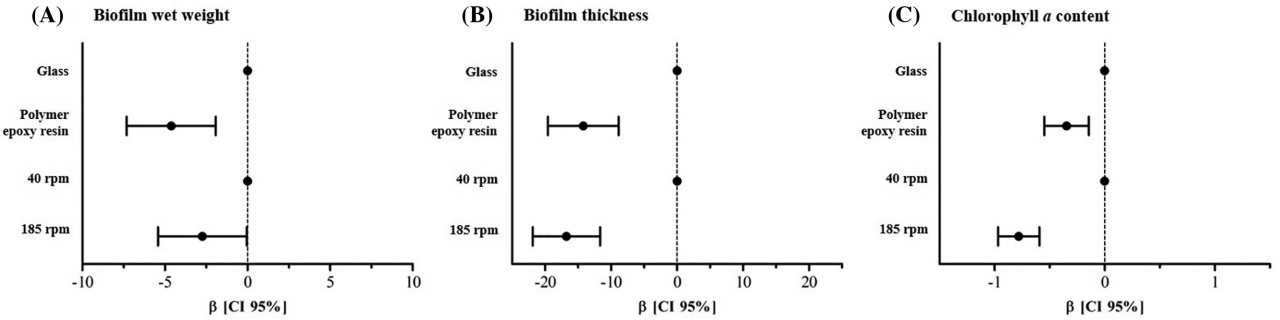

Figure 2. Associations between biofilm wet weight **(A)**, thickness **(B)** and chlorophyll *a* content **(C)** and the independent variables. Glass and 40 rpm were used as the reference conditions. LRMs were adjusted for strain and incubation periods. Results are presented as beta estimates (β) and the corresponding 95% confidence interval (CI 95%).

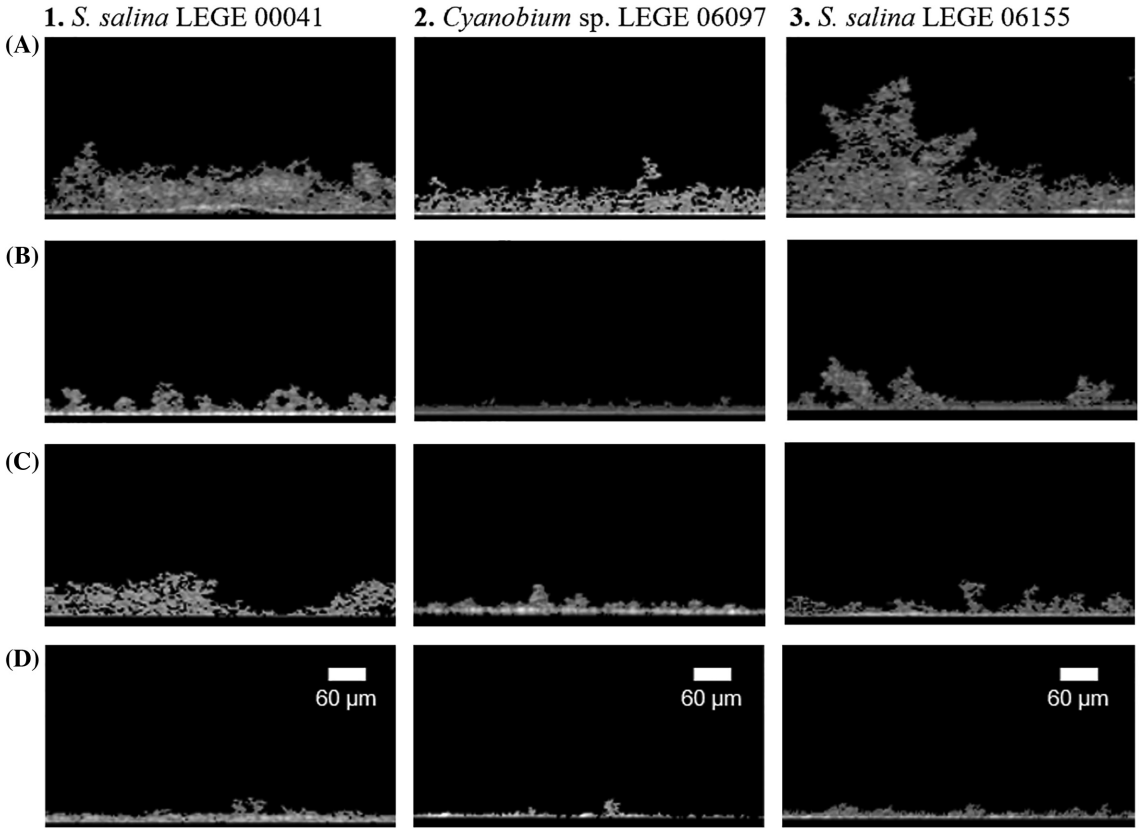

Figure 3. Representative images of biofilm structures captured on day 42 using OCT for *S. salina* LEGE 00041 (1), *Cyanobium* sp. 06097 (2) and *S. salina* 06155 (3) biofilms formed on glass at 40 and 185 rpm (**A** and **B**, respectively) and on polymer epoxy resin at 40 and 185 rpm (**C** and **D**, respectively).

about the course of biofilm formation regardless of the microorganism type. Indeed, this is possible since microbial adhesion is one of the first steps of biofilm formation, involving physicochemical and molecular interactions (Di Martino 2018).

The adhesion of living microorganisms to a surface is a complex process affected by multiple factors. It is known that surface properties, including the hydrophobicity, influence the cell adhesion and subsequent biofilm formation (Zhang *et al.* 2015; Spengler *et al.* 2019). In this study, the results of theoretical adhesion models classified the glass surface as hydrophilic and the polymer epoxy resin surface as hydrophobic. In addition, the calculation of the free energy of adhesion indicated that the cyanobacteria cell adhesion on glass is thermodynamically unfavourable, while being favourable on polymer epoxy resin surfaces. However, our experimental results showed that for all tested cyanobacteria, the number of both adhered and biofilm cells was higher for glass than for a polymer epoxy resin surface. Although a considerable number of studies indicate that hydrophobic surfaces are favourable for bacterial adhesion (Cerca *et al.* 2005; De-la-Pinta *et al.* 2019) and, in particular, for cyanobacterial adhesion (Ozkan and Berberoglu 2013), other studies found no correlation between surface hydrophobicity and cell attachment (Mazumder *et al.* 2010; Irving and Allen 2011; Faria *et al.* 2020; Talluri *et al.* 2020). These contradictory results may be explained by the existence of conditioning films formed due to the adsorption of (macro)molecules on the substrate that change the adhesion conditions for microorganisms (Lorite *et al.* 2011; Hwang *et al.* 2012). The nature of films is related to the

material type and the environment that surrounds them (e.g. growth medium and type of microorganism) (Lorite *et al.* 2011; Talluri *et al.* 2020). Besides, it was described that conditioning films form a few minutes after the surfaces are exposed, with subsequent growth for several hours, playing an important role in cyanobacteria adhesion and in the early stages of biofilm formation (Talluri *et al.* 2020). Thus, despite the physicochemical properties of the surfaces being fundamental (Zhang *et al.* 2015), the cyanobacterial adhesion and biofilm formation may be modulated by other factors.

The hydrodynamic conditions have also been pointed out as an important modulating factor of cyanobacterial adhesion and biofilm formation (Romeu *et al.* 2019; Faria *et al.* 2020) being able to change protein expression (Romeu *et al.* 2020). Similar to what happens for initial attachment of other microfoulers (Nolte *et al.* 2017), our data demonstrated that the number of cyanobacteria cells that adhered to surfaces was higher at 40 than 185 rpm. This result was observed for both adhesion and biofilm formation assays, which indicated that shear forces have an influence not only in the early stages of biofilm formation but also during maturation stages. Indeed, higher shear forces may hamper initial cell attachment and facilitate the detachment of adhered microorganisms during biofilm formation (Thomen *et al.* 2017).

Microbial adhesion is also affected by the physicochemical properties of the microorganisms (Zhang *et al.* 2015). The thermodynamic characterisation of cyanobacterial cells indicated that *S. salina* LEGE 00041 is relatively more hydrophobic than the other cyanobacteria. Indeed, a higher number of adhered and biofilm cells was registered for *S. salina* LEGE 00041 compared with *Cyanobium* sp. LEGE 06097 and *S. salina* LEGE 06155. Although the association between initial adhesion and biofilm formation has been verified for the three cyanobacteria, they behaved differently regardless of their taxonomic order. For this reason, and to obtain further knowledge, this association was investigated using LRMs adjusted for the microorganism and incubation periods. According to the LRMs, the initial cell adhesion assays were able to estimate that: (i) biofilms formed on glass displayed a higher number of cells than those formed on polymer epoxy resin; and (ii) biofilms formed at 40 rpm exhibited a higher number of cells than those formed at 185 rpm. Moreover, a significant correlation was found between the number of cells at the end of the initial adhesion period and the number of biofilm cells on day 42. In addition, the latter depends on the initial adhesion and hydrodynamic conditions.

These results were corroborated by analysis of the different biofilm parameters, with biofilms developed on glass displaying higher values of biofilm wet weight, thickness and chlorophyll *a* content compared to biofilms formed on the polymer epoxy resin surface. Likewise, biofilms formed at 40 rpm also exhibited higher wet weight, thickness and chlorophyll *a* content.

The potential of the initial adhesion assays to estimate the biofilm formation was also confirmed by the OCT analysis. Indeed, cyanobacterial biofilms formed on glass were thicker than those formed on the polymer epoxy resin. Also, biofilms formed at 40 rpm presented a more developed structure than at 185 rpm.

Overall, initial cell adhesion assays revealed a high potential to estimate biofilm development by cyanobacteria. Although thermodynamic studies provide important information about the surface properties and the interaction between surfaces and microorganisms, adhesion assays are crucial since biofilm formation is a complex process that involves a multiplicity of extrinsic factors. Thus, initial adhesion assays performed by cell counting after 7.5 h incubation allow high throughput screening of marine coatings considering different conditions (e.g. hydrodynamic forces and microorganisms type), providing indications about the biofilm behaviour in a short time. Therefore, this approach may be useful as a screening tool for marine coatings development, avoiding, at the first stage, the extensive laboratory assays monitoring biofilm parameters for long periods (6–8 weeks) or field trials often performed without prior evidence of a coating's effectiveness. Nevertheless, further research is needed to ensure that these short-term adhesion assays may be applied to a broader range of marine-engineered surfaces.

SUPPLEMENTARY DATA

Supplementary data are available at *FEMSEC* online.

FUNDING

This work was supported by Base Funding UIDB/00511/2020 of the Laboratory for Process Engineering, Environment, Biotechnology and Energy—LEPABE—funded by national funds through the FCT/MCTES (PIDDAC), 'CVMAR+I—Industrial Innovation and Marine Biotechnology Valorization' project, funded by INTERREG V Espanha Portugal (POCTEP) (0302_CVMAR_I_1_P), and project UIDB/04423/2020. R.T.-S. acknowledges receipt of a junior researcher fellowship from the Project PTDC/BII-BIO/29589/2017—POCI-01–0145-FEDER-029589—funded by FEDER funds through COMPETE2020–Programa Operacional Competitividade e Internacionalização (POCI) and by national funds (PIDDAC) through FCT/MCTES.

Conflicts of interest. None declared.

REFERENCES

Akinfijevs T, Janvaevskis A, Lavendelis E. *A Brief Survey of Ship Hull Cleaning Devices*. Latvia: RTU, 2007.

Alves P, Gomes LC, Vorobii M *et al.* The potential advantages of using a poly(HPMA) brush in urinary catheters: effects on biofilm cells and architecture. *Colloids Surf B* 2020;**191**:110976.

Amara I, Miled W, Slama RB *et al.* Antifouling processes and toxicity effects of antifouling paints on marine environment. A review. *Environ Toxicol Pharmacol* 2018;**57**:115–30.

Angelova AG, Ellis GA, Wijesekera HW *et al.* Microbial composition and variability of natural marine planktonic and biofouling communities from the Bay of Bengal. *Front Microbiol* 2019;**10**:2738.

Arrhenius A, Backhaus T, Hilvarsson A *et al.* A novel bioassay for evaluating the efficacy of biocides to inhibit settling and early establishment of marine biofilms. *Mar Pollut Bull* 2014;**87**: 292–9.

Azevedo J, Antunes JT, Machado AM *et al.* Monitoring of biofouling communities in a Portuguese port using a combined morphological and metabarcoding approach. *Sci Rep* 2020;**10**:13461.

Azevedo NF, Pacheco AP, Keevil CW *et al.* Adhesion of water stressed Helicobacter pylori to abiotic surfaces. *J Appl Microbiol* 2006;**101**:718–24.

Bakker DP, van der Plaats A, Verkerke GJ *et al.* Comparison of velocity profiles for different flow chamber designs used in studies of microbial adhesion to surfaces. *Appl Environ Microbiol* 2003;**69**:6280.

Basu S, Hanh BM, Isaiah CJQ *et al.* Green biolubricant infused slippery surfaces to combat marine biofouling. *J Colloid Interface Sci* 2020;**568**:185–97.

Bayoudh S, Othmane A, Bettaieb F *et al*. Quantification of the adhesion free energy between bacteria and hydrophobic and hydrophilic substrata. *Mater Sci Eng C* 2006;**26**:300–05.

Blain S, Guillou J, Treguer P *et al*. High frequency monitoring of the coastal marine environment using the MAREL buoy. *J Environ Monit* 2004;**6**:569–75.

Brian-Jaisson F. *Identification et caractérisation des exopolymères de biofilms de bactéries marines*. Toulon: Université de Toulon, 2014.

Briand JF. Marine antifouling laboratory bioassays: an overview of their diversity. *Biofouling* 2009;**25**:297–311.

Busscher HJ, Weerkamp AH, van der Mei HC *et al*. Measurement of the surface free energy of bacterial cell surfaces and its relevance for adhesion. *Appl Environ Microbiol* 1984;**48**:980–3.

Cerca N, Pier GB, Vilanova M *et al*. Quantitative analysis of adhesion and biofilm formation on hydrophilic and hydrophobic surfaces of clinical isolates of Staphylococcus epidermidis. *Res Microbiol* 2005;**156**:506–14.

De-la-Pinta I, Cobos M, Ibarretxe J *et al*. Effect of biomaterials hydrophobicity and roughness on biofilm development. *J Mater Sci: Mater Med* 2019;**30**:77.

de Carvalho CCCR. Marine biofilms: a successful microbial strategy with economic implications. *Front Mar Sci* 2018;**5**:126.

Di Martino P. Bacterial adherence: much more than a bond. *AIMS Microbiology* 2018;**4**:563–6.

Faria Sara I, Teixeira-Santos R, Romeu MJ *et al*. The relative importance of shear forces and surface hydrophobicity on biofilm formation by coccoid cyanobacteria. *Polymers* 2020;**12**:653.

Flemming HC, Murthy PS, Venkatesan R *et al*. *Marine and Industrial Biofouling*. In: William Costerton J (ed.). Heidelberg, Germany: Springer, 2009, 4.

Georgiades E, Kluza D. Evidence-based decision making to underpin the thresholds in New Zealand's craft risk management standard: biofouling on vessels arriving to New Zealand. *Mar Technol Soc J* 2017;**51**:76–88.

Gomes LC, Deschamps J, Briandet R *et al*. Impact of modified diamond-like carbon coatings on the spatial organization and disinfection of mixed-biofilms composed of Escherichia coli and Pantoea agglomerans industrial isolates. *Int J Food Microbiol* 2018;**277**:74–82.

Gomes LC, Silva LN, Simões M *et al*. Escherichia coli adhesion, biofilm development and antibiotic susceptibility on biomedical materials. *J Biomed Mater Res A* 2015;**103**:1414–23.

Hwang G, Kang S, El-Din MG *et al*. Impact of conditioning films on the initial adhesion of Burkholderia cepacia. *Colloids Surf B* 2012;**91**:181–8.

Irving TE, Allen DG. Species and material considerations in the formation and development of microalgal biofilms. *Appl Microbiol Biotechnol* 2011;**92**:283–94.

Janczuk B, Chibowski E, Bruque JM *et al*. On the consistency of surface free energy components as calculated from contact angles of different liquids: an application to the cholesterol surface. *J Colloid Interface Sci* 1993;**159**:421–8.

King RK, Flick GJ, Smith SA *et al*. Comparison of bacterial presence in biofilms on different materials commonly found in recirculating aquaculture systems. *J Appl Aquaculture* 2006;**18**:79–88.

Kotai J. *Instructions for Preparation of Modified Nutrient Solution Z8 for Algae*. Oslo: Norwegian Institute for Water Research, 1972, 5.

Lacoursière-Roussel A, Bock DG, Cristescu ME *et al*. Effect of shipping traffic on biofouling invasion success at population and community levels. *Biological Invasions* 2016;**18**:3681–95.

Leroy C, Delbarre-Ladrat C, Ghillebaert F *et al*. A marine bacterial adhesion microplate test using the DAPI fluorescent dye: a new method to screen antifouling agents. *Lett Appl Microbiol* 2007;**44**:372–8.

Lopez-Mila B, Alves P, Riedel T *et al*. Effect of shear stress on the reduction of bacterial adhesion to antifouling polymers. *Bioinspiration Biomimetics* 2018;**13**:065001.

Lorite GS, Rodrigues CM, de Souza AA *et al*. The role of conditioning film formation and surface chemical changes on Xylella fastidiosa adhesion and biofilm evolution. *J Colloid Interface Sci* 2011;**359**:289–95.

Ma Y, Cao X, Feng X *et al*. Fabrication of super-hydrophobic film from PMMA with intrinsic water contact angle below 90°. *Polymer* 2007;**48**:7455–60.

Mazumder S, Falkinham JO, Dietrich AM *et al*. Role of hydrophobicity in bacterial adherence to carbon nanostructures and biofilm formation. *Biofouling* 2010;**26**:333–9.

McClay T, Zabin C, Davidson I *et al*. *'Vessel Biofouling Prevention And Management Options Report, U.S*. Coast Guard R&D Center, 2015.

Meireles A, Fulgêncio R, Machado I *et al*. Characterization of the heterotrophic bacteria from a minimally processed vegetables plant. *LWT - Food Sci Technol* 2017;**85**:293–300.

Minchin D, Gollasch S. Fouling and ships' hulls: how changing circumstances and spawning events may result in the spread of exotic species. *Biofouling* 2003;**19**:111–22.

Neves AR, Almeida JR, Carvalhal F *et al*. Overcoming environmental problems of biocides: synthetic bile acid derivatives as a sustainable alternative. *Ecotoxicol Environ Saf* 2020;**187**:109812.

Nolte KA, Schwarze J, Beyer CD *et al*. Parallelized microfluidic diatom accumulation assay to test fouling-release coatings. *Biointerphases* 2018;**13**:041007.

Nolte KA, Schwarze J, Rosenhahn A. Microfluidic accumulation assay probes attachment of biofilm forming diatom cells. *Biofouling* 2017;**33**:531–43.

Oss CJ van. *Interfacial forces in aqueous media*. New York: Marcel Dekker Inc., 1994.

Ozkan A, Berberoglu H. Cell to substratum and cell to cell interactions of microalgae. *Colloids Surf B* 2013;**112**:302–9.

Porra RJ, Thompson WA, Kriedemann PE. Determination of accurate extinction coefficients and simultaneous equations for assaying chlorophylls a and b extracted with four different solvents: verification of the concentration of chlorophyll standards by atomic absorption spectroscopy. *Biochim Biophys Acta - Bioenergetics* 1989;**975**:384–94.

Rajeev M, Sushmitha TJ, Prasath KG *et al*. Systematic assessment of chlorine tolerance mechanism in a potent biofilm-forming marine bacterium Halomonas boliviensis. *Int Biodeterior Biodegrad* 2020;**151**:104967.

Ramos V, Morais J, Castelo-Branco R *et al*. Cyanobacterial diversity held in microbial biological resource centers as a biotechnological asset: the case study of the newly established LEGE culture collection. *J Appl Phycol* 2018;**30**:1437–51.

Romeu MJ, Alves P, Morais J *et al*. Biofilm formation behaviour of marine filamentous cyanobacterial strains in controlled hydrodynamic conditions. *Environ Microbiol* 2019;**21**:4411–24.

Romeu MJL, Domínguez-Pérez D, Almeida D *et al*. Characterization of planktonic and biofilm cells from two filamentous cyanobacteria using a shotgun proteomic approach. *Biofouling* 2020;**36**:631–45.

Salta M, Wharton JA, Stoodley P *et al*. Designing biomimetic antifouling surfaces. *Philos Trans A Math Phys Eng Sci* 2010;**368**:4729–54.

Schultz MP, Bendick JA, Holm ER *et al*. Economic impact of biofouling on a naval surface ship. *Biofouling* 2011;**27**: 87–98.

Selim MS, Shenashen MA, El-Safty SA *et al*. Recent progress in marine foul-release polymeric nanocomposite coatings. *Prog Mater Sci* 2017;**87**:1–32.

Spengler C, Nolle F, Mischo J *et al*. Strength of bacterial adhesion on nanostructured surfaces quantified by substrate morphometry. *Nanoscale* 2019;**11**:19713–22.

Stafslien S, Daniels J, Mayo B *et al*. Combinatorial materials research applied to the development of new surface coatings IV. A high-throughput bacterial biofilm retention and retraction assay for screening fouling-release performance of coatings. *Biofouling* 2007;**23**: 45–54.

Stafslien SJ, Bahr J, Daniels J *et al*. High-throughput screening of fouling-release properties: an overview. *J Adhes Sci Technol* 2011;**25**:2239–53.

Talluri SNL, Winter RM, Salem DR. Conditioning film formation and its influence on the initial adhesion and biofilm formation by a cyanobacterium on photobioreactor materials. *Biofouling* 2020;**36**:183–99.

Taylor DA. Chapter 16 - Engineering materials. In Taylor DA (ed). *Introduction to Marine Engineering (Second Edition)*. Oxford, UK: Butterworth-Heinemann, 1996, 326–40.

Telegdi J, Trif L, Románszki L. 5 - Smart anti-biofouling composite coatings for naval applications. In: Montemor MF (ed). *Smart Composite Coatings and Membranes*. Cambridge, UK: Woodhead Publishing, 2016, 123–55.

Thomen P, Robert J, Monmeyran A *et al*. Bacterial biofilm under flow: first a physical struggle to stay, then a matter of breathing. *PLoS One* 2017;**12**:e0175197.

Tian L, Yin Y, Jin H *et al*. Novel marine antifouling coatings inspired by corals. *Mater Today Chem* 2020;**17**:100294.

Wendt DE. Methods of assessing antifouling and foul-release efficacy of non-toxic marine coatings. *Green Mater* 2017;**5**: 22–30.

Zecher K, Aitha VP, Heuer K *et al*. A multi-step approach for testing non-toxic amphiphilic antifouling coatings against marine microfouling at different levels of biological complexity. *J Microbiol Methods* 2018;**146**:104–14.

Zhang X, Zhang Q, Yan T *et al*. Quantitatively predicting bacterial adhesion using surface free energy determined with a spectrophotometric method. *Environ Sci Technol* 2015;**49**:6164–71.